

Supplementary Information

**Determination of partial conductivities and computational analysis of
theoretical power density of BaZr_{0.1}Ce_{0.7}Y_{0.1}Yb_{0.1}O_{3-δ} (BZCYYb1711)
electrolyte under idiomatic PCFC conditions**

*In-Ho Kim¹, Dae-Kwang Lim², Hohun Bae¹, Aman Bhardwaj¹, Jun-Young Park³ and Sun-
Ju Song^{1,*}*

¹Ionics Lab, Department of Materials Science and Engineering, Chonnam National
University, 77, Yongbong-ro, Buk-gu, Gwang-Ju, 61186, Republic of Korea

²Applied Science Research Institute, Korea Advanced Institute of Science and Technology,
Daejeon 34141, Republic of Korea

³HMC, Department of Nanotechnology and Advanced Materials Engineering, Sejong
University, Seoul 143-747, South Korea

*Corresponding Author: Prof. Sun-Ju Song

Mailing address: Department of Materials Science and Engineering, Chonnam National
University, 77 Yongbong-ro, Buk-gu, Gwang-Ju, 61186, Republic of Korea

E-mail address: song@chonnam.ac.kr

Partial Conductivity

The defect structure of the BCY-BZY system was well described in a previous study. In this BZCYYb1711 system, the Schottky–Wagner defect equilibrium was ignored because the errors resulting from this omission are negligible for heavily-doped systems.¹ Thus, the charge neutrality condition can be given as follows (details in previous studies^{2,3})

$$n + [Y,Yb_{Ce,Zr}] = p + 2[V_{O}^{\bullet\bullet}] + [OH_{O}^{\bullet}] \quad (S1)$$

$$\frac{1}{2}O_{2(g)} + V_{O}^{\bullet\bullet} \Leftrightarrow O_{O}^x + 2h^{\bullet}; K_{OX} = \frac{p^2}{[V_{O}^{\bullet\bullet}]P_{O_2}^{1/2}} \quad (S2)$$

$$H_2O_{(g)} + V_{O}^{\bullet\bullet} + O_{O}^x \Leftrightarrow 2OH_{O}^{\bullet}; K_H = \frac{[OH_{O}^{\bullet}]^2}{[V_{O}^{\bullet\bullet}]P_{H_2O}} \quad (S3)$$

The partial conductivities of each of the charge carriers can be written in terms of the product of the concentration and diffusivity of the mobile defect species as follows

$$\sigma_{OH_{O}^{\bullet}} = \sigma_{OH_{O}^{\bullet}}^* \left[\left(1 + \frac{\alpha}{p_{H_2O}} \right)^{1/2} - 1 \right] \left(\frac{p_{H_2O}}{\alpha} \right) \left(\frac{\alpha}{(1 + \alpha)^{1/2} - 1} \right) \quad (S4)$$

$$\sigma_{V_{O}^{\bullet\bullet}} = \sigma_{V_{O}^{\bullet\bullet}}^* \left[\left(1 + \frac{\alpha}{p_{H_2O}} \right)^{1/2} - 1 \right]^2 \left(\frac{p_{H_2O}}{\alpha} \right) \quad (S5)$$

$$\sigma_p = \sigma_p^* \left[\left(1 + \frac{\alpha}{p_{H_2O}} \right)^{1/2} - 1 \right] \left(\frac{p_{H_2O}}{\alpha} \right)^{1/2} p_{O_2}^{1/4} \quad (S6)$$

where the conductivity at standard partial pressures was selected, $\sigma_{OH_{O}^{\bullet}}^*$ represents the protonic

conductivity at $p_{H_2O} = 1$ atm, σ_p^* is the hole conductivity at $p_{O_2} = 1$ atm and $p_{H_2O} = 0$ atm,

and $\sigma_{V\ddot{O}}^*$ is the oxygen-ion conductivity when $[V\ddot{O}]$ is independent of p_{O_2} and $p_{H_2O} = 0$ atm.

Here, $\sigma_p \propto p_{H_2O}^{1/2} p_{O_2}^{-1/4}$. Parameter α is a constant determined as follows

$$\alpha = \frac{8[Y, Yb_{Ce, Zr}]}{K_w} \quad (S7)$$

where $[Y, Yb_{Ce, Zr}] = \frac{x \cdot N_A}{V_m}$, in which x is the molar dopant concentration, N_A is Avogadro's number, and V_m is the molar volume of the system. By considering the charge neutrality conditions (S8) and the relation between conductivities and concentrations (S9), the partial conductivities of each species could be determined as given below⁴.

$$2[V\ddot{O}] + [OH\dot{O}] + p = [Y_B'] \quad (S8)$$

$$\sigma_i = z_i c_i \mu_i = \frac{z_i F}{V} [C_i] \mu_i \quad (S9)$$

$$\sigma_{OH\dot{O}} = \frac{F}{4V} \mu_{OH\dot{O}} K_H p_{H_2O} \left[\sqrt{\left(1 + \frac{K_H^{1/2} p_{O_2}^{1/4}}{K_O^{1/2} p_{H_2O}^{1/2}}\right)^2 + \frac{8[Y_B']}{K_H p_{H_2O}}} - \left(1 + \frac{K_H^{1/2} p_{O_2}^{1/4}}{K_O^{1/2} p_{H_2O}^{1/2}}\right) \right] \quad (S10)$$

$$\sigma_p = \frac{F}{4V} \mu_p \frac{K_H^{3/2}}{K_O^{1/2}} p_{H_2O}^{1/2} p_{O_2}^{1/2} \left[\sqrt{\left(1 + \frac{K_H^{1/2} p_{O_2}^{1/4}}{K_O^{1/2} p_{H_2O}^{1/2}}\right)^2 + \frac{8[Y_B']}{K_H p_{H_2O}}} - \left(1 + \frac{K_H^{1/2} p_{O_2}^{1/4}}{K_O^{1/2} p_{H_2O}^{1/2}}\right) \right] \quad (S11)$$

$$\sigma_{V_O^{\bullet\bullet}} = \frac{F}{8V} \mu_{V_O^{\bullet\bullet}} K_H p_{H_2O} \left[\sqrt{\left(1 + \frac{K_H^{1/2} p_{O_2}^{1/4}}{K_O^{1/2} p_{H_2O}^{1/2}}\right)^2 + \frac{8[Y_B']}{K_H p_{H_2O}}} - \left(1 + \frac{K_H^{1/2} p_{O_2}^{1/4}}{K_O^{1/2} p_{H_2O}^{1/2}}\right) \right]^2 \quad (S12)$$

$$\sigma_T = \sigma_{OH_O^{\bullet}} + \sigma_{V_O^{\bullet\bullet}} + \sigma_p \quad (S13)$$

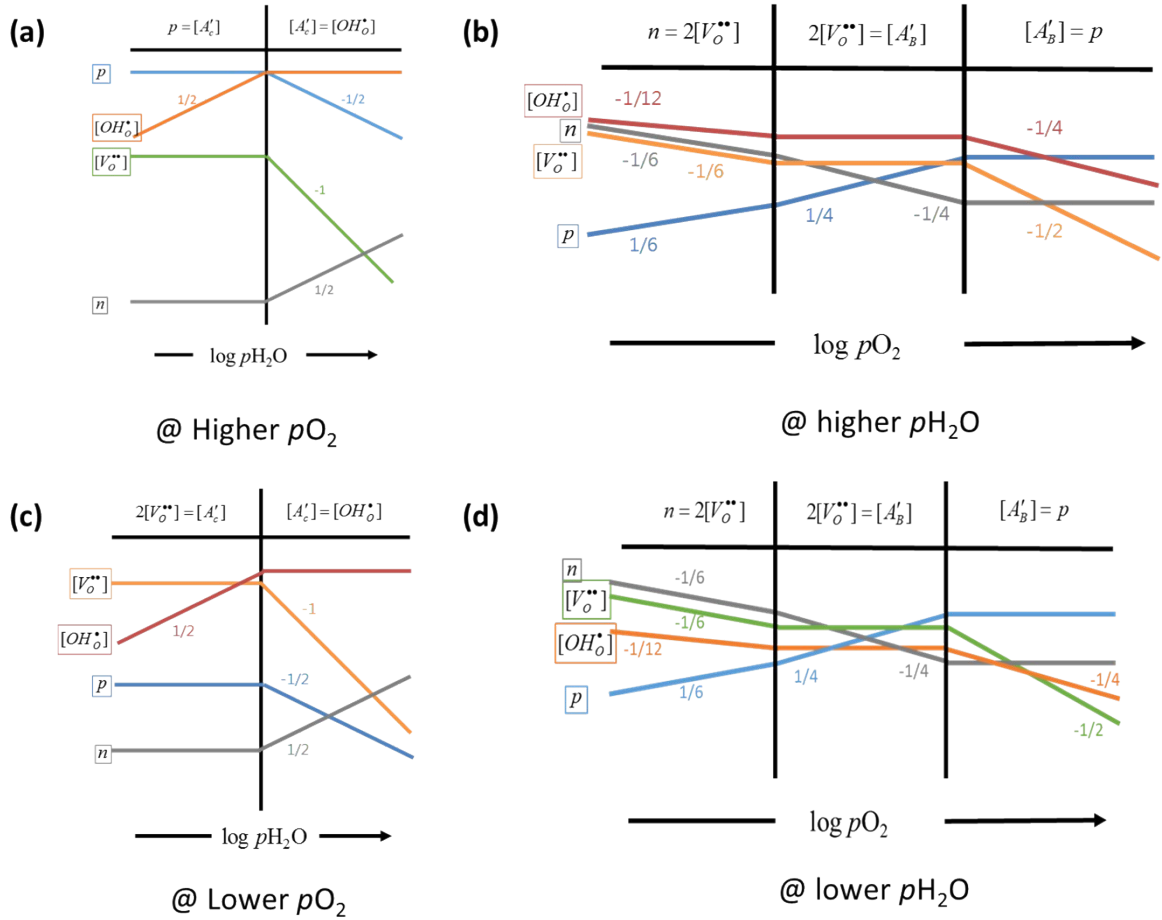


Fig. S1. Defect equilibrium diagrams of BZCYYb1711 as a function of p_{H_2O} at (a) higher p_{O_2} and (b) lower p_{O_2} and as a function of p_{O_2} at (c) higher p_{H_2O} and (d) lower p_{H_2O} .

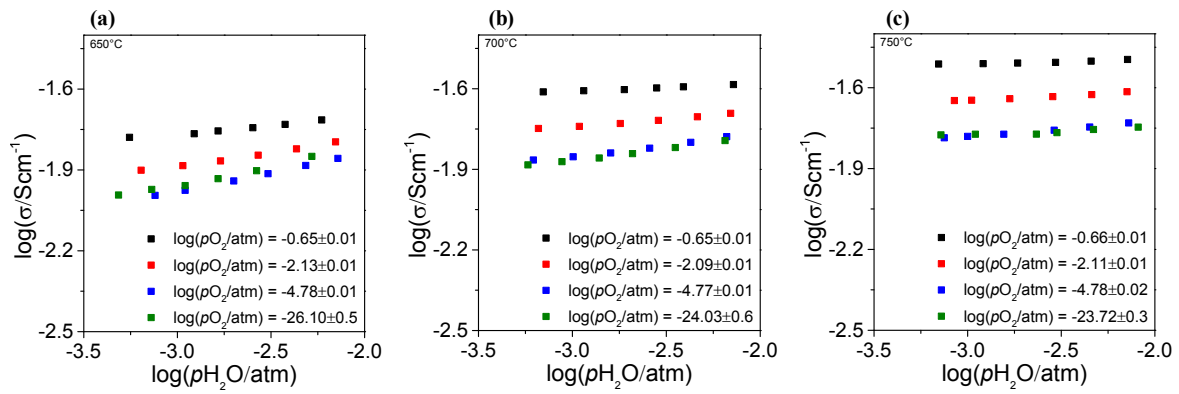


Fig. S2. Total conductivity of BZCYYb1711 electrolyte as a function of water vapor pressure at (a) 650 °C, (b) 700 °C, and (c) 750 °C.

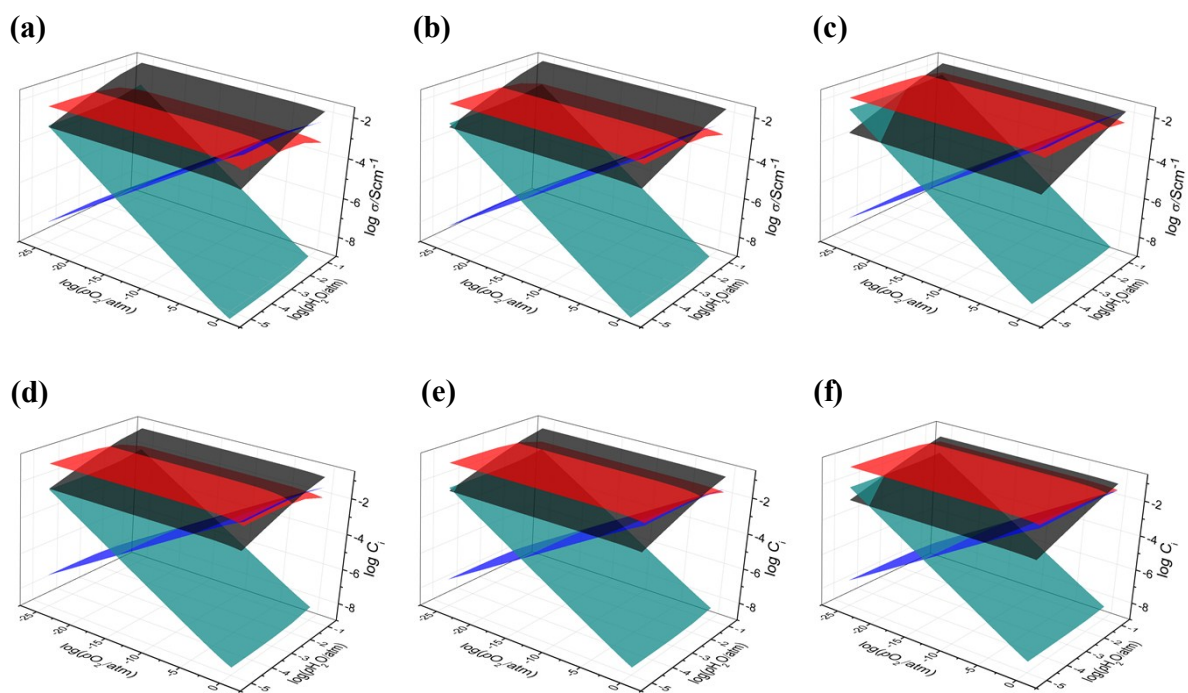


Fig. S3. 3D diagrams of Partial conductivities of BZCYYb1711 at (a) 650 °C, (b) 700 °C, and (c) 750 °C. Concentrations of mobile charge carriers at (a) 650 °C, (b) 700 °C, and (c) 750 °C. Here, each mobile charge carrier is denoted as- black is proton, red is oxygen, blue is hole, and dark cyan is electron.

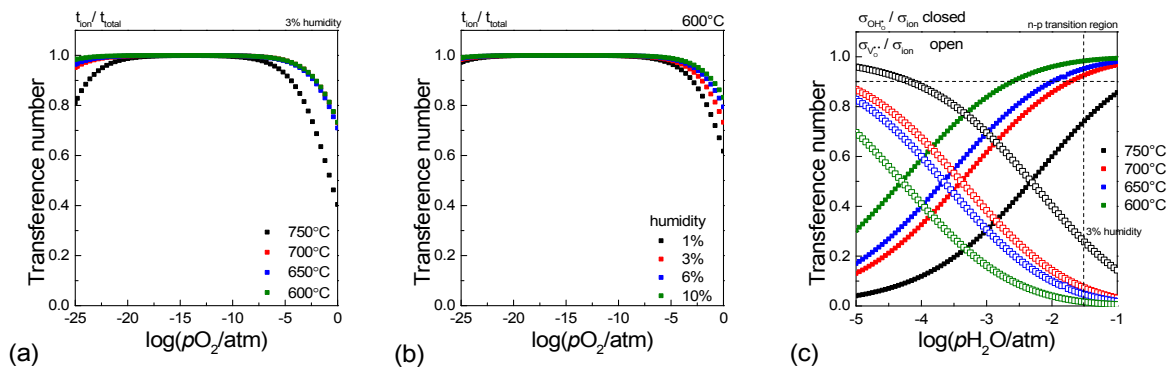


Fig. S4. Ratio of $t_{\text{ion}}/t_{\text{total}}$ as a function of (a) temperature and (b) humidity; (c) Proton dominant regime ($t_{\text{proton}} \geq 0.9$) at $p\text{H}_2\text{O}/\text{atm} \geq 0.03$.

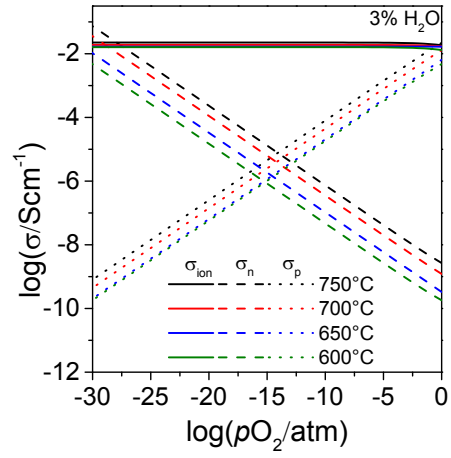


Fig. S5. Partial conductivity and N-P transition point of BZCYYb1711 as a function of pO_2 in the temperature range of 600 – 750 °C.

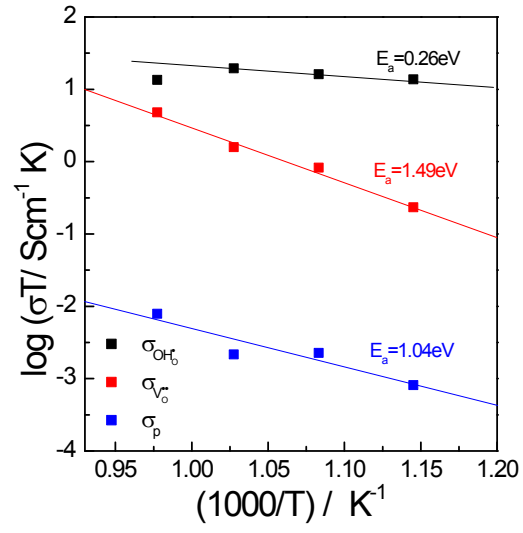


Fig. S6. Arrhenius curves of the partial conductivities of BZCYYb1711 and their activation energies

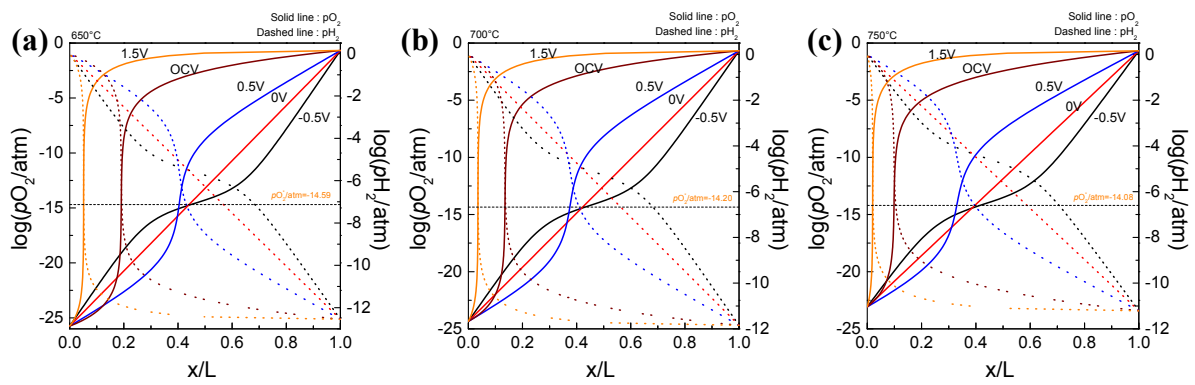


Fig. S7. Spatial distributions of chemical potential gradient of BZCYYb1711 under 3% humidified air at air electrode and 3% humidified hydrogen at fuel electrode at (a) 650 °C, (b) 700 °C, and (c) 750 °C.

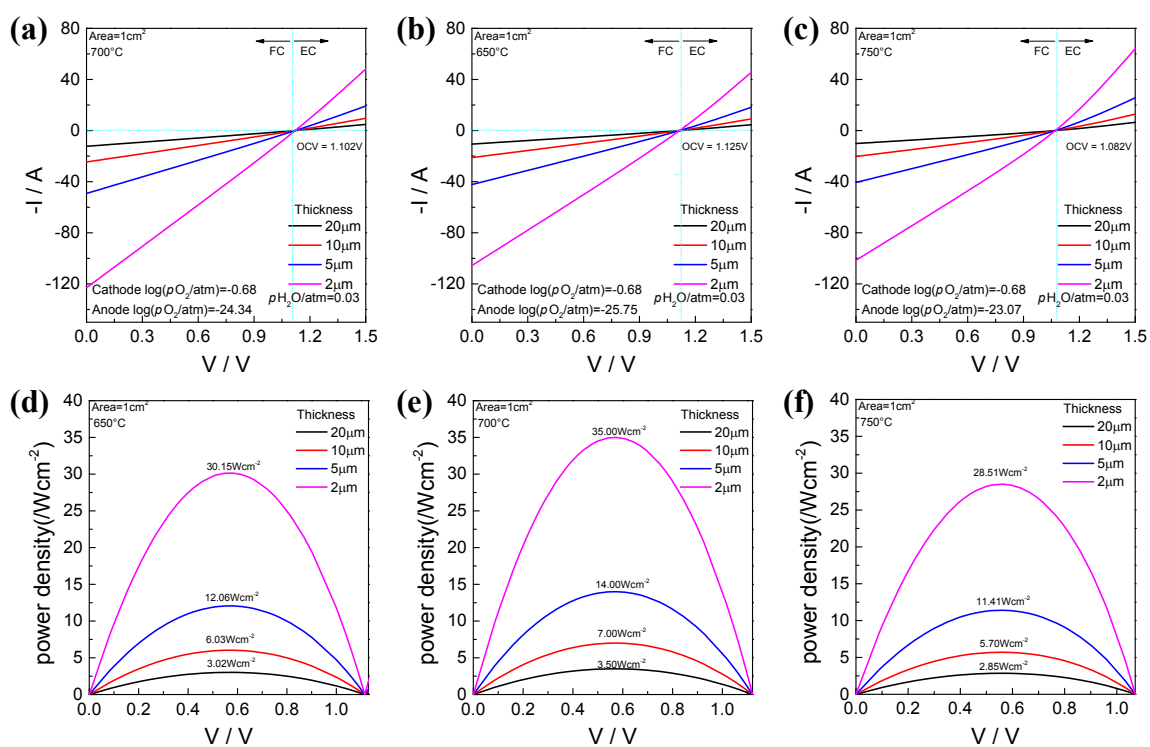


Fig. S8. I-V profiles (a,b,c) and power densities (d,e,f) of BZCYYb1711 with various electrolyte thicknesses at (a,d) 650 °C, at (b,e) 700 °C, and (c,f) 750 °C under the supply of 3% humidified air/hydrogen gas to each electrode.

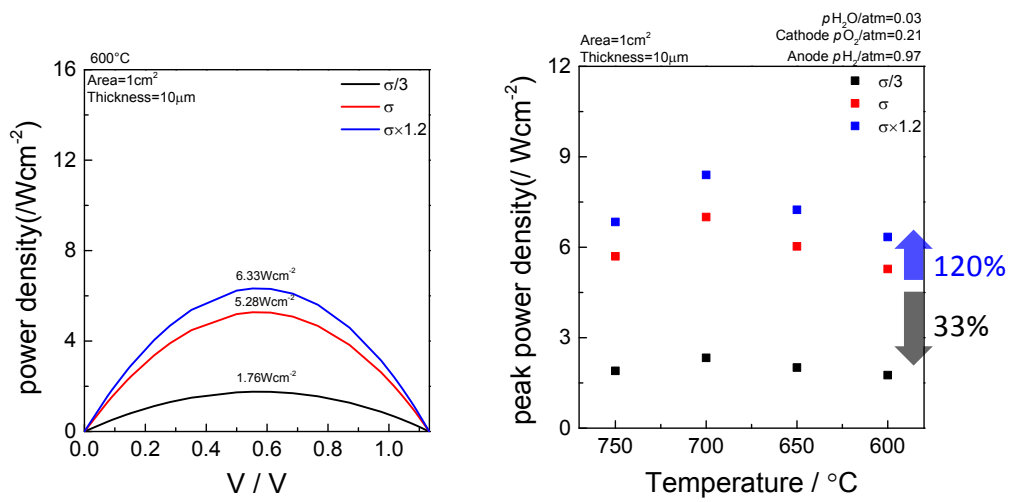


Fig. S9. (a) Theoretical power density at 600°C and (b) peak power densities at different operating temperatures for BZCYYb1711 considering 1/3 times lower and 1.2 times higher values of calculated total conductivities.

Table S1. Theoretical peak power density of BZCYYb1711 as a function of hydrogen with various water vapor pressures in fuel electrode and gas type with 3% humidity in air electrode at 600 °C.

Gas condition @ anode side	Thickness (μm)	Air condition @ cathode side (W/cm^2)	Oxygen condition @ cathode side (W/cm^2)
3% humidified hydrogen	10	5.27	5.55
	20	2.64	2.78
	30	1.76	1.85
4% humidified hydrogen	10	5.34	5.63
	10	5.38	5.66
5% humidified hydrogen	20	2.69	2.83
	30	1.79	1.89
	10	5.39	5.68
6% humidified hydrogen	10	5.39	5.68
7% humidified hydrogen	10	5.40	5.68
8% humidified hydrogen	10	5.39	5.68
9% humidified hydrogen	10	5.38	5.67
10% humidified hydrogen	10	5.37	5.66
	20	2.69	2.83
	30	1.79	1.89

Reference

1. N. Bonanos, F. W. Poulsen. Considerations of Defect Equilibria in High Temperature Proton-Conducting Cerates, *J. Mater. Chem.* 9 (1999) 431-434.
2. D.-K. Lim, M.-B. Choi, K.-T. Lee, H.-S. Yoon, E. D. Wachsman, S.-J. Song, Non-Monotonic Conductivity Relaxation of Proton-conducting $\text{BaCe}_{0.85}\text{Y}_{0.15}\text{O}_{3-\delta}$ upon Hydration and Dehydration, *Int. J. Hydrog. Energy* 36 (2011) 9367-9373.
3. S.-J. Song, E. D. Wachsman, S. E. Dorris, U. Balachadran, Electrical Properties of p-type Electronic Defects in the Protonic Conductor $\text{SrCe}_{0.95}\text{Eu}_{0.05}\text{O}_{3-\delta}$, *J. Electrochem. Soc.* 150 (2003) A790-A795.
4. E. Kim, Y. Yamazaki, S. M. Hail, H.-Y. Yoo, Effect of NiO sintering-aid on hydration kinetics and defect-chemical parameters of $\text{BaZr}_{0.8}\text{Y}_{0.2}\text{O}_{3-d}$, *Solid State Ionics* 275 (2015) 23-28.